Sorption of Uranium (VI) From Aqueous Solution Using Nanomagnetite Particles; Singly and Coated With Humic Acid

Ismail Mohamed Ahmed (imibrahim@ju.edu.sa)
Egyptian Atomic Energy Authority
Aly A. Helal
Egyptian Atomic Energy Authority
Rasha Gamal
Egyptian Atomic Energy Authority
Salah aboEinien
Ain Shams University Faculty of Science
Abdullah A. Helal
Egyptian Atomic Energy Authority

Research Article

Keywords: Sorption, Nanomagnetite, Humic acid coated nanomagnetite, Uranium (VI)

Posted Date: December 6th, 2021

DOI: https://doi.org/10.21203/rs.3.rs-1052562/v1

Abstract

Magnetite nanoparticles (Fe_3O_4) and humic acid coated magnetite nanoparticles (Fe_3O_4/HA) were investigated for the removal of U(VI) from aqueous solution. Batch sorption experiments were studied as a function contact time, adsorbent mass, U(VI) concentration and pH. The sorption kinetic data follow the pseudo-second order while the isotherms are found to obey Langmuir model with maximum capacity (Q_{max}) of 230, 196 mg/g for Fe_3O_4 and Fe_3O_4/HA, respectively. The study reveals that humic acid decreases the sorption capacity due to the formation of a polyanionic organic coating and thus altering the surface properties of the particles and reduces the magnetite aggregation and stabilizes the magnetite suspension.

1. Introduction

Nuclear activities produce hazardous wastes that are varying in their source, chemical composition, physical state, in addition to their radioactivity. The waste coming from the nuclear facilities is very toxic and carcinogenic as it contains U(VI) ions that implies good practice in radioactive waste management to protect living organisms and the environment from radiation. Numerous methods are used for the removal of uranium and its fission products from surface and groundwater, and waste streams. The World Health Organization (WHO) has reported the maximum amount of uranium in drinking water as 0.2ppm (**WHO 2018**). Many techniques were proposed to eliminate the radionuclides from liquid wastes as ion exchange, liquid-liquid extraction, precipitation and adsorption. Ion exchange and adsorption techniques are the most effective methods as they characterized by their simplicity and low operating costs (**Chandra and Fahmida 2020; Hossein et al. 2014**). Many adsorbents as clay minerals, polymers and biomass showed low sorption capacity that limit their use (**Wang et al., 2018).** Recently, magnetic nanoparticles have drawn attention due to their large surface area, little internal diffusion resistance, high stability, shape-controlled, and narrow size distribution. Several methods for their synthesis were reported as co-precipitation, thermal decomposition, microemulsion, solvothermal, microwave-assisted and laser pyrolysis. The surface of the magnetite nanoparticles have modified using various coating materials including organic polymer, organic surfactants, inorganic oxides and bioactive molecules to improve their efficiency (**Pragnesh and Lakhan 2014; Ngenefeme et al. 2013; Grazhulene et al., 2018; Helal, 2018)**. In this concern, humic acid (HA) showed high affinity to Fe_3O_4 nanoparticles and prevent their accumulation. The aim of this work is focused on the investigation of the sorption behavior of uranium ions onto magnetite nanoparticles (Fe_3O_4) and humic acid coated magnetite nanoparticles (Fe_3O_4/HA).

2. Experimental

2.1. Reagents and instrumentation

All chemicals used were of analytical grade and used without any further purification.

The microstructure of the Fe_3O_4 and Fe_3O_4/HA was investigated by FTIR Spectrometer (a Nicolet spectrometer from Meslo, USA). Mineralogical analysis of the sample was determined by XRD using a Shimadzu-6000, Japan) diffractometer. The surface morphology of Fe_3O_4 and Fe_3O_4/HA is investigated by transmission electron microscope (TEM). pH meter of the Hanna instruments type was used to monitored the hydrogen ion concentration for the solutions. In the sorption experiments, a good mixing of the two phases was achieved by using a

thermostated shaker of the type Julapo (Germany). The concentration of uranium were estimated using Shimadzu UV/Vis, double beam recording spectrophotometer, Model 160-A, Japan .

2.3. Synthesis of magnetite nanoparticles and humic acid coated magnetite nanoparticles

The two investigated adsorbents were prepared by co-precipitation method. Briefly, $FeCl_3$ and $FeSO_4.7H_2O$. were mixed with a molar ratio 2:1 at 80^0C, then precipitated by1.0 M NaOH, drop by drop, with vigorous stirring under nitrogen atmosphere. The black precipitate was collected and washed several times with distilled water and dried. The humic acid coated nanomagnetite was synthesized by adding humic acid (0.5 g/L) was dissolved in concentrated ammonia and added Fe^{3+} and Fe^{2+} (2:1) mixture, drop by drop, under nitrogen atmosphere until black precipitate is obtained that was collected, washed and dried.

2.4 Batch adsorption procedure

In the batch experiments, 5.0 mg from both Fe_3O_4 and Fe_3O_4/HA were shaken with 20 mL from U(VI) ions with initial concentration of 50 ppm for 2.0 h, at pH 7.0, 5.5 respectively, and 25^{o}C unless otherwise stated. The sorbents were separated by using a magnet, and the solution was centrifuged for U(VI) measurement by UV-Vis spectrophotometer using Arsenazo(III) method (**Marzenko 1986**). The percent uptake was calculated as follow:

$$Uptake\% = (C_i - C_f) / C_i * 100 \quad (1)$$

Where C_i and C_f are the initial and final concentration, respectively.

3. Results And Discussion

3.1 Characterization of Sorbents

Figure 1 shows the phase composition of the magnetite and humic acid coated nanoparticles were analyzed by XRD. The Fe_3O_4 particles show peaks at 2θ values of 30.22, 35.6, 42.4, 58.4, 62.78 and which are characteristic for the magnetite spinel structure (**Sun et al.2007**).

The chemical structure of adsorbent was determined by FTIR, Fig. 2a,b shows a characteristic band for Fe3O4 at 570 cm^{-1}due to Fe –O stretching band (**Carlos et al. 2012**) that confirms the presence of the magnetic core. The absorption peak at about 3400 cm^{-1} is originated by hydroxyls (OH) while bands at 2925 and 1396 cm-1is most likely due to the stretching CH and CH_2 scissoring in humic acid. The coating of Fe_3O_4 by HA is confirmed by presence of bands in (Fig. c), at ~ 1620 cm $^{-1}$which is due to C = O stretching, indicating that the carboxylate anion interacts with the FeO surface (**Yantasee et al. 2007**).

The surface morphology of Fe_3O_4 and Fe_3O_4/HA was investigated by transmission electron microscope (TEM). The image of TEM was shown in (Fig. 3a, b) where most of the magnetite nanoparticles were found to be quasi-spherical with a mean size around 15 nm. The improvement in the dispersion may be due to that the HA weaken the interaction between the magnetite particles.

3.2. Sorption study

3.2.1. Effect of pH

In order to explain the sorption behavior and mechanism of the aqueous species of U (VI), the distribution species of U (VI) as a function of pH was calculated. The effect of pH was investigated in the range 2.5-7 on Fe_3O_4 and in the range 2.5-6 in case of Fe_3O_4/HA. As pH increases with the pH of the solution, Fig. 4. The relative distribution of aqueous U (VI) species in solution at a concentration of 2×10^{-4} mol/L is presented in Fig. 5, using Visual MINTEQ ver. 3.0.33l (**Gustafsson 2012**). It is clear that the soluble uranyl hydroxo complex $(UO_2)_3(OH)_5^+$ and $(UO_2)_4(OH)_7^+$ are the predominant species at pH range 5.0-7.0 that favors the interaction betwee the functional groups that exist at magnetite surface (=FeOOH) in addition to the presence of carboxylic and phenolic group on humic acid (**Li and Kaplan 2012**).

3.2.2. Sorption kinetics

Kinetic investigations were performed to elucidate the mechanism of adsorption of metal ions, explain how fast the rate of chemical reaction occurs and also to know the factors affecting the reaction rate. Among them three kinetic models (the Lagergren's pseudo-first order kinetic model, pseudo-second order model and intraparticle diffusion models) were used for examination of our experimental data.

The pseudo first order equation was suggested by Lagergren, for the adsorption of solid-liquid systems. It is generally expressed as follows:

$$\log(q_e - q_t) = \log q_e - (\frac{k_1}{2.303})t (2)$$

The sorption data were also investigated by pseudo second order mechanism. In this model, the rate-limiting step is the surface adsorption that involves chemisorption (**Ahmed et al 2017**).The pseudo-second-order adsorption kinetic rate equation is expressed as:

$$\left(\frac{t}{q_t}\right)=\left(\frac{1}{k_2 q_e^2}\right)+\left(\frac{1}{q_e}\right)t \quad (3)$$

Where q_e and q_t (mg/g) refer to the amount of metal ions adsorbed on both adsorbents at equilibrium and at time (t), respectively. k_1 is the rate constant of pseudo first order (min^{-1}) while k_2 (gmg^{-1} min^{-1}) is the rate constant of the second-order adsorption.

The rate constants were calculated and tabulated in Table (1). As the calculated equilibrium sorption shows, capacity (q_e) from second-order kinetic model is consistent with the experimental data, Table (1). Therefore, the sorption can be described by pseudo second order kinetic model, Fig. 6a, b, c.

The intraparticle diffusion model is expressed as the following equation:

$q_t = k_i t^{1/2} + C$ (4)

Where k_3 ($mg\ g^{-1}\ min^{-0.5}$) is the intra-particle diffusion rate constant and C is the intercept which is proportional to the boundary layer thickness, Fig. 6c. The linear relationships that do not pass through the origin point that infers the intraparticle diffusion is not the dominant mechanism in processes occurring during the sorption of U(VI) ions on Fe_3O_4 and Fe_3O_4/ HA and other mechanisms such as film diffusion or particle diffusion may control the sorption process (**Jaeshik et al. 2012**) and the parameters are listed in Table (1).

3.2.3. Isotherm models

In this study, three isotherm models were tested to find the best fitting equations such as: Langmuir and Freundlich models. In Langmuir isotherm model, the linear form is represented by the following equation:

$$\frac{1}{Q_e} = \frac{1}{Q_m} + \frac{1}{K_L Q_m C_e} \quad (5)$$

Where, q_e is the amount adsorbed (mg/g), C_e is the equilibrium concentration of the metal ion (mg/L), and Q^o and b are Langmuir constants related to the adsorption capacity and binding energy between the adsorbent and the adsorbate, respectively. These constants can be calculated by plotting of C_e/q_e against C_e. The results are illustrated in Fig. (7a,b) and Table (2).

The linear equation of Freundlich model is commonly represented as:

$\log q_e = \log K_f + (1/n)\log Ce$ (6)

Where K_f and n are the Freundlich constants characteristics of the system, indicating the adsorption capacity and the adsorption intensity, respectively that were estimated from the plot of $\log q_e$ versus $\log C_e$, Fig. (8a,b) and tabulated in Table (2). The R^2 values for the Langmuir equation in case of the two investigated adsorbents are higher than those obtained from the Freundlich equation.

A comparison of the adsorption performance of Fe_3O_4 and Fe_3O_4/HA with other adsorbents was reported in Table 3. The results implied that the investigated adsorbents can used efficiently for the uptake of U(VI) from aqueous medium.

4. Conclusion

In this study, magnetite nanoparticles and magnetite coated with humic acid were prepared, characterized and applied for uranium ions removal. The maximum capacity is 196.0 mg/g for Fe_3O_4/ HA, and 230.0 mg/g for Fe_3O_4. The humic acid decreases the capacity, as it cause a polyanionic organic coating and thus altering the surface properties of the particles.

Declarations

Author contribution: Conceptualization: Ismail Mohamed Ahmed ,Aly Helal , Rasha Gamal, Salah Abo-El-Enein , Abdullah Helal. Investigation: Rasha Gamal. Writing—original draft: Rasha Gamal . Writing—review and editing: Ismail Mohamed Ahmed ,Aly A. Helal , Salah Abo-El-Enein , Abdullah A. Helal.

Funding: Not applicable

Availability of data and materials: The authors can confirm that all relevant data are included in the article, mentioned in the reference list.

Ethics approval : Not applicable.

Consent to participate: Not applicable.

Consent to publish: Not applicable. This manuscript does not involve individuals that may object to having their data published in a journal article.

Competing interests: The authors declare no competing interests

References

1. Ahmed I, Gamal R, Helal Aly., Abo-El-Enein S, Helal, A (2017) Kinetic Sorption Study of Cerium (IV) on Magnetite Nanoparticles. Part. Sci. Technol. 35(6):643-652. https://doi.org/10.1080/02726351.2016.1192572
2. Baumann N, Brendler V, Arnold T, Geipel G, Bernhard, G (2005) Uranyl sorption onto gibbsite studied by time-resolved laser induced fluorescence spectroscopy (TRLFS). J Colloid Interf Sci 290: 318-324. https://doi.org/10.1016/j.jcis.2004.10.076
3. Carlos L, Cipollone M, Soria D, Moreno M, Ogillby P, Einschlag, F, Martire D (2012) The effect of humic acid binding to magnetite nanoparticles on the photogeneration of reactive oxygen species. Sep. Purif. Technol. 91:23–29. DOI: 10.1016/j.seppur.2011.08.028
4. Chandra C, Fahmida K (2020) Nano-scale zerovalent copper: green synthesis, characterization and efficient removal of uranium. J. Radioanal. Nucl. Chem. 324:589–597. https://doi.org/10.1007/s10967-020-07080-1
5. Ding Y, Xian Q, Wang E, He X, Jiang Z, Dan H, Zhu W (2020) Mesoporous MnO_2/SBA-15 as a synergetic adsorbent for enhanced uranium adsorption. New J. Chem. 44: 13707-13715. https://doi.org/10.1039/D0NJ02966A
6. Donat R and Aytas S (2005) Adsorption and thermodynamic behavior of uranium(VI) on Ulva sp.-Na bentonite composite. J Radioanal Nucl Chem. 265:107-112. Doi 10.1007/s10967-005-0794-6
7. Fan F, Qin Z, Bai J, Rong W, Fan F, Tian W, Wu X, Wang Y, Zhao L (2012) Rapid removal of uranium from aqueous solutions using magnetic Fe_3O_4@SiO_2 composite particles. J Environ Radioact. 106: 40-46. DOI: 10.1016/j.jenvrad.2011.11.003
8. Fasfous I and Dawoud J(2012) Uranium (VI) sorption by multiwalled carbon nanotubes from aqueous solution. Appl Surf Sci. 259:433-440. DOI: 10.1016/j.apsusc.2012.07.062
9. Gustafsson J (2012) Visual MINTEQ ver. 3.3. Department of Land and Water Resources Engineering, KTH (Royal Institute of Technology), SE-100 44, Stockholm, Sweden. Available at http:// www2.lwr.kth.se/English/OurSoftware/vminteq/index.htm
10. Grazhulene S, Zolotareva N , Red'kin A, ShilkinaN, Mitina A, Kolesnikova A (2018) Magnetic Sorbent Based on Magnetite and Modified Carbon Nanotubes for Extraction of Some Toxic Elements. Russian Journal of Applied Chemistry volume 91:1849–1855. DOI: 10.1134/S1070427218110162
11. Helal A, Mazario E, Mayoral A, Decorse, P, Losno R, Lion, C, Hémadi, M (2018) Highly efficient and selective extraction of uranium from aqueous solution using a magnetic device: succinyl-β-cyclodextrin-APTES@maghemite nanoparticles. Environmental Science: Nano, 5(1): 158–168. Doi:10.1039/c7en00902j
12. Hossein F, Mohammad M, Alireza F, Mozhgan I (2014) Evaluation of a new magnetic zeolite composite for removal of Cs^+ and Sr^{2+} from aqueous solutions: Kinetic, equilibrium and thermodynamic studies. Comptes Rendus Chimie. 17(2): 108-117 . DOI: 10.1016/j.crci.2013.02.006
13. Jaeshik C, Jinyoung C, Jinwoo L, Sang, L, Seok, W (2012) Sorption of Pb (II) and Cu (II) onto multi-amine grafted mesoporous silica embedded with nano-magnetite: Effects of steric factors. J. Hazard Mater. 239:183-189. DOI: 10.1016/j.jhazmat.2012.08.063

14. Li D, Kaplan, D (2012) Literature Review on the Sorption of Plutonium, Uranium, Neptunium, Americium, and Technetium to Corrosion Products on Waste Tank Liners" SRNL-STI-2012-00040, Savannah River National Laboratory
15. Marzenko Z (1986) Spectrophotometric Determination of Elements, John Wiley and Sons Inc., New York.
16. Ngenefeme F, Namanga J., Yufanyi D, Ndinteh D, KrauseW (2013) A One Pot Green synthesis and characterisation of iron oxide-pectin hybrid nanocomposite. OJCM 3:30-37. DOI:10.4236/ojcm.2013.32005
17. Pragnesh N and Lakhan V (2014) Application of iron oxide nanomaterials for the removal of heavy metals. J. nanotechnol. 2014:1-14. https://doi.org/10.1155/2014/398569
18. Schleuter D, Silvia, A, Zoran H, Hanke, T, Bernhard, G, Brunner, E (2013) Chitin based renewable materials from marine sponges for uranium adsorption. Carbohydr. Polym. 92, 712-720. Doi: 10.1016/j.carbpol.2012.08.090
19. Sun J, Zhou, S, Hou P, Yang Y, Weng, J, Li X, Li M (2007) Synthesis and characterization of biocompatible Fe_3O_4 nanoparticles. J Biomed Mater Res A. 80A (2):333–341. Doi: 10.1002/jbm.a.30909
20. Tian, G., Geng, J., Jin, Y., Wang, C., Li, S., Chen, Z., Wang, H., Zhao, Y., Li, S (2011) Sorption of uranium(VI) using oxime-grafted ordered mesoporous carbon CMK-5. J Hazard Mater. 190, 422-450. https://doi.org/10.1016/j.jhazmat.2011.03.066
21. Wang S, Guo W, Gao F, Wang Y, Gao Y (2018) Lead and uranium sorptive removal from aqueous solution using magnetic and nonmagnetic fast pyrolysis rice husk biochars. RSC Adv 8:13205-13210. https://doi.org/10.1039/C7RA13540H
22. WHO (2008) Guidelines for drinking-water quality: second addendum. Vol. 1, Recommendations.
23. Xia L, Tan K, Wang X, Zheng, W (2013) Uranium Removal from Aqueous Solution by Banyan Leaves: Equilibrium, Thermodynamic, Kinetic, and Mechanism Studies. J. Environ. Eng. 139:887-894. DOI: 10.1061/(ASCE)EE.1943-7870.0000695
24. Yakout S, Metwally S, El-Zakla T (2013) Uranium sorption onto activated carbon prepared from rice straw: Competition with humic acids. Appl. Surf. Sci. 280: 745- 750. DOI: 10.1016/j.apsusc.2013.05.055
25. Yang A, Wang Z, Zhu Y (2018) Facile preparation and highly efcient sorption of magnetic composite graphene oxide/Fe_3O_4/ GC for uranium removal . Scientifc Reports. 11:8440-8450 https://doi.org/10.1038/s41598-021-86768-0
26. Yantasee W, Warner C, Sangvanich T, Addleman R, Carter T, Wiacek R, Fryxell G, Timchalk C,M. Warner M (2007) Removal of heavy metals from aqueous systems with thiol functionalized superparamagnetic nanoparticles. Environmental Science & Technology 41:5114–19. Doi:10.1021/es0705238
27. Zhao G, Wen T, Yang X, Yang S, Liao J, Shao D, Wang X (2012) Preconcentration of U(VI) ions on few-layered graphene oxide nanosheets from aqueous solutions. Dalton Trans. 41: 6182-6188. https://doi.org/10.1039/C2DT00054G
28. Zong P, Wang S, Zhao Y, Wang H, Pan H, He C (2013) RETRACTED: High sorption of U(VI) on graphene oxides studied by batch experimental and theoretical calculation. Chem Eng. J. 220: 45-52. DOI: 10.1016/j.cej.2015.11.066

Tables

Table 1
Comparison of the pseudo first, second-order and intra-particle diffusion constants, calculated and experimental q_e values, for U (VI) ions onto Fe_3O_4 and Fe_3O_4/ HA

Adsorbent	*First-order kinetic parameters*			*Second-order kinetic parameters*			Intra-particle diffusion			q_e, exp. (mg/g)
	k_1 ($min.^1$)	q_e,calc. (mg/g)	R^2	k_2 (g/mg.min)	q_e, calc. (mg/g)	R^2	k_i (mg g^{-1} $min^{-0.5}$)	C	R^2	
Fe_3O_4	0.034	78.1	0.97	1.32×10^{-3}	117.7	0.998	1.5	25	0.996	116
Fe_3O_4/HA	0.025	46.6	0.95	1.21×10^{-3}	158	0.999	1.2	107	0.994	155.6

Table 2 : Langmuir and Freundlich parameters for the sorption of U(VI) on both Fe_3O_4 and Fe_3O_4/HA

Adsorbent	*Langmuir parameters*			*Freundlich parameters*			q_e, exp. (mg/g)
	b (L/mg)	$Q^0_{max.}$ (mg/g)	R^2	n	K_f (mg/g)	R^2	
Fe_3O_4	0.12	238	0.999	3.75	57	0.964	230
Fe_3O_4/HA	0.11	195.6	0.999	5.37	82	0.930	196

Table 3: Comparison of sorption capacities for U(VI) using various adsorbent materials

Sorbent	Q_{max}, mg/g	Optimum pH	Ref.
Oxime-grafted mesoporous carbon	65.18	4.5	(Tian et al., 2012)
Chitin based marine sponges	288.0	7.0	(Schleuter et al., 2013)
Rice straw (AC)	100.0	5.5	(Yakout et al., 2013)
Banyan leaves	22.06	3.0	(Xia et al., 2013)
Graphine oxide	97.5	5.0	(Zhao et al., 2012)
Fe_3O_4-GO	69.49	5.5	(Zong et al., 2013)
Mesoporous MnO_2/SBA-15	465.1	6.0	(Ding et al., 2020]
MWCNTs	39.5	5.0	(Fasfous and Dawoud, 2012
Fe_3O_4 Silica coated -coated NPs	52.4	6.0	(Fan et al., 2012)
Nano magnetite	230.0	7.0	(This study)
Nano magnetite coated HA	196.0	5.0	(This stud)

Figures

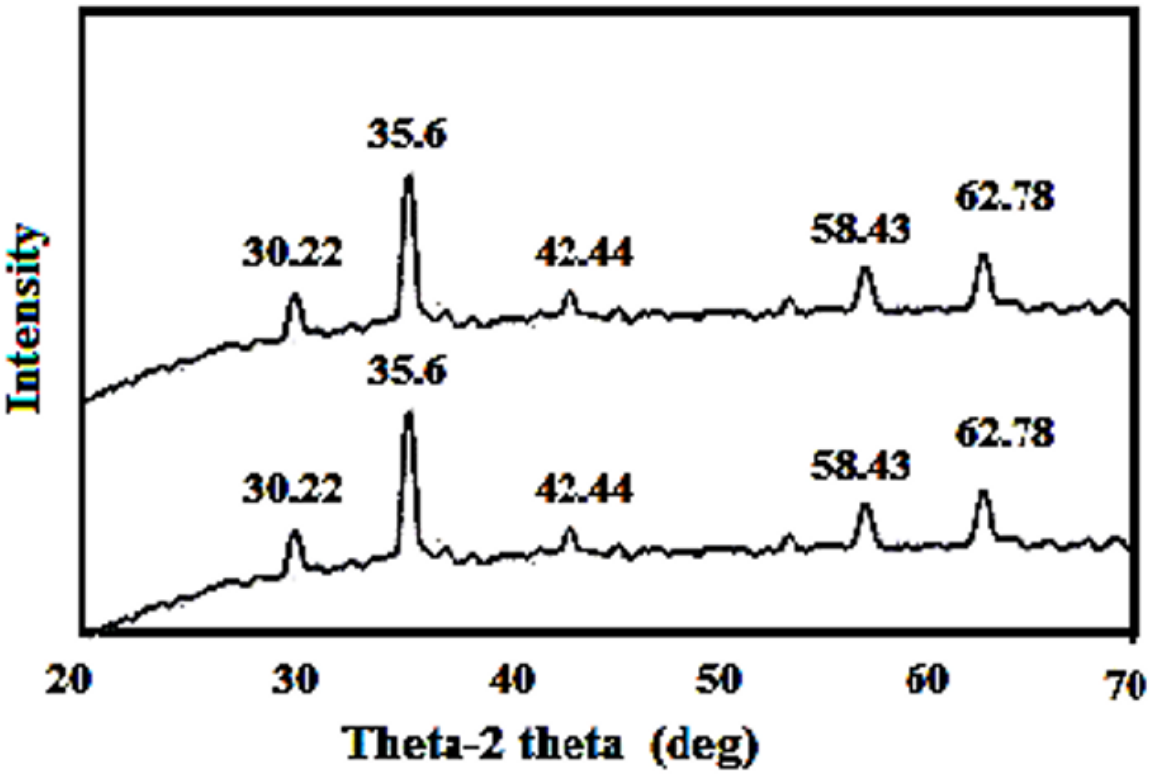

Figure 1

XRD of Fe3O4 and Fe3O4/ HA nanoparticles

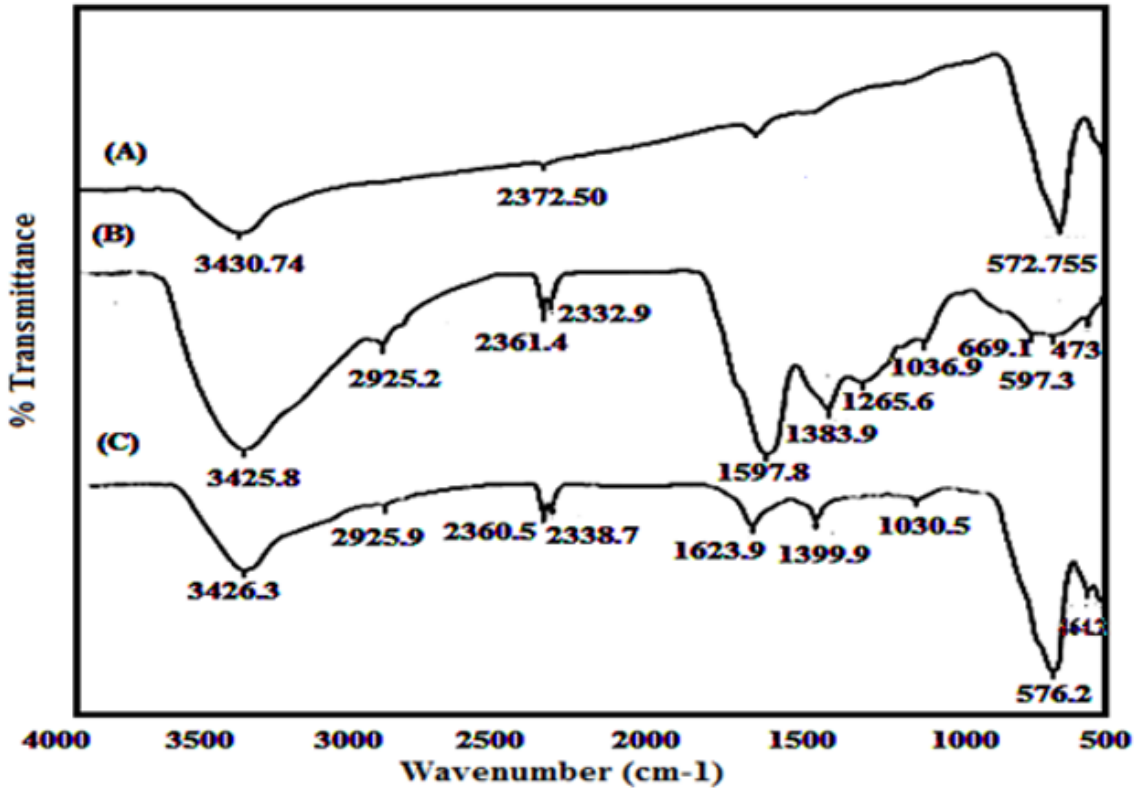

Figure 2

IR spectra of (A) magnetite nanoparticles (B) Humic acid (C) humic acid coated magnetite nanoparticles.

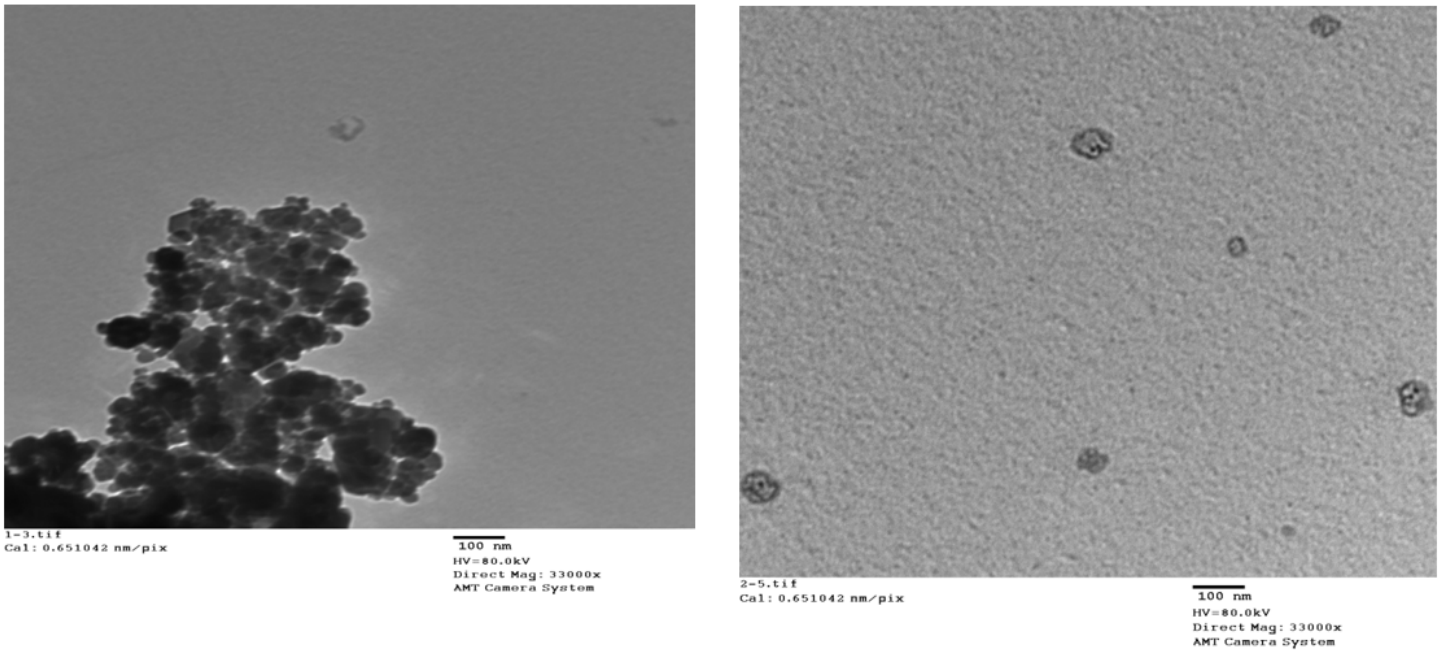

Figure 3

a): TEM image for Fe3O4 nanoparticles b): TEM image for Fe3O4/ HA nanoparticles

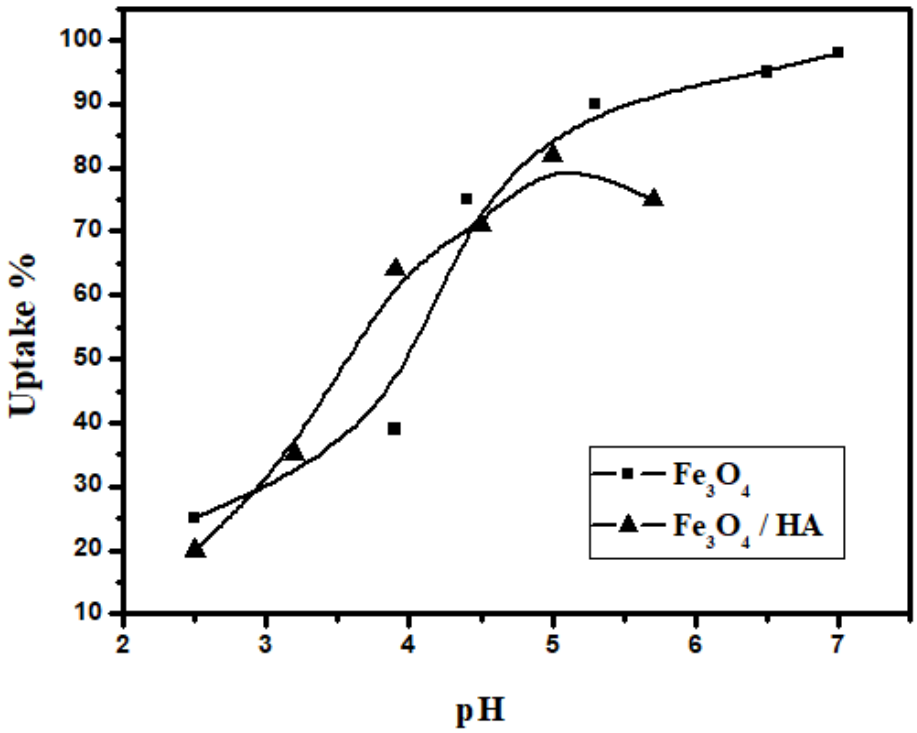

Figure 4

Effect of pH on the sorption of UO22+ by Fe3O4 and Fe3O4/HA

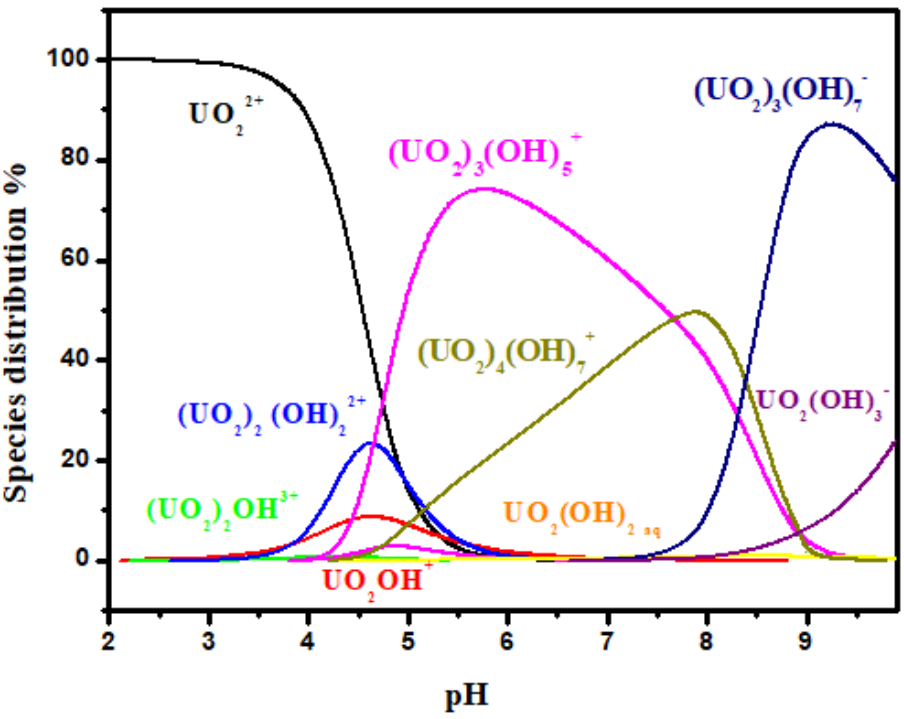

Figure 5

Species distribution of uranyl ions

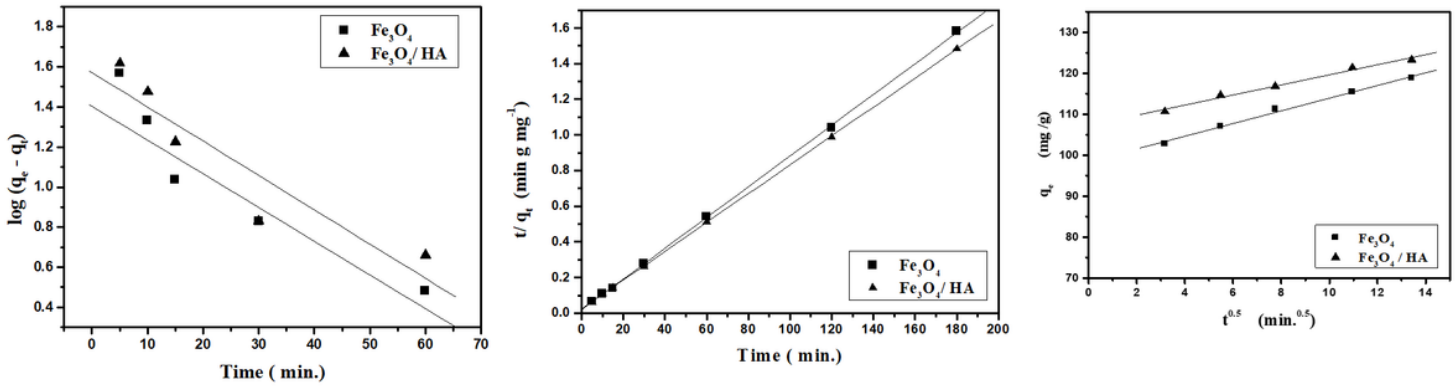

Figure 6

a): Pseudo- first order plot for the sorption of U(VI) on Fe3O4 and Fe3O4/ HA b): Pseudo- second-order plot for the sorption of U(VI) on Fe3O4 and Fe3O4/ HA c): Intra-particle diffusion for the sorption of U(VI) on Fe3O4 and Fe3O4/HA

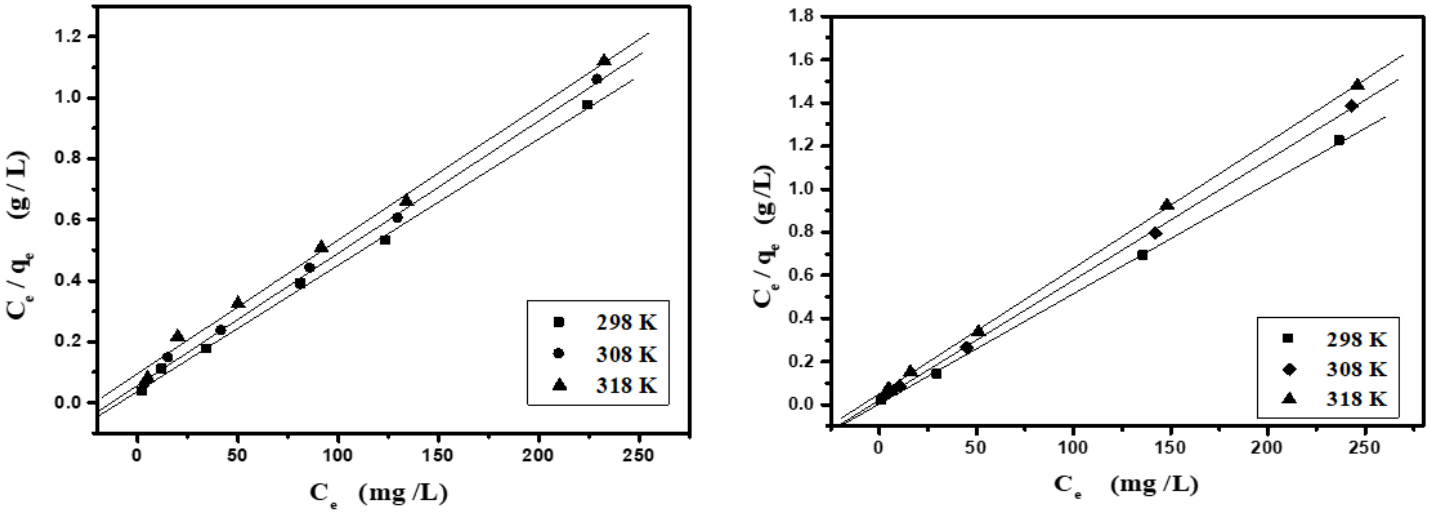

Figure 7

(a): Langmuir plot for the sorption of U(VI) on Fe3O4 at different temperatures (b): Langmuir plot for the sorption of U(VI) on Fe3O4/ HA at different temperatures

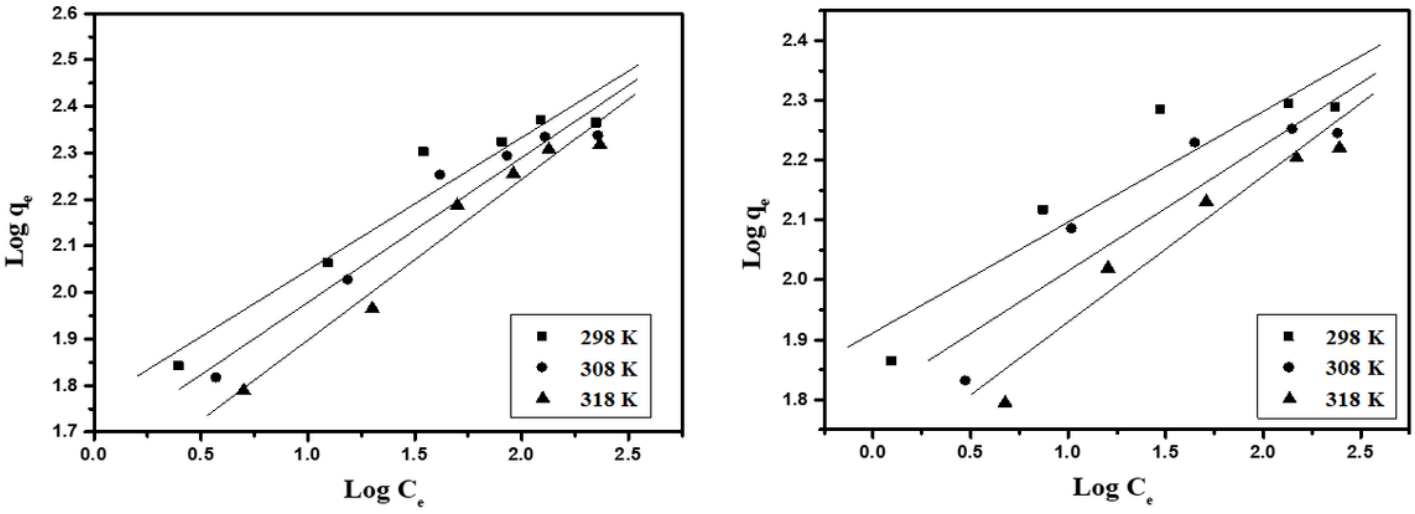

Figure 8

a): Freundlich plot for the sorption of U(VI) on Fe3O4 at different temperatures b): Freundlich plot for the sorption of U(VI) on Fe3O4/ HA at different temperatures